Mineralogical Magazine (2024), **88**, 90–96
doi:10.1180/mgm.2023.86

CAMBRIDGE UNIVERSITY PRESS

Article

Bimbowrieite, $NaMgFe_5^{3+}(PO_4)_4(OH)_6{\cdot}2H_2O$, a new dufrénite-group mineral from the White Rock No.2 quarry, South Australia, Australia

Peter Elliott[1,2] and Anthony R. Kampf[3]

[1]School of Physics, Chemistry and Earth Sciences, The University of Adelaide, Adelaide, South Australia 5005, Australia; [2]South Australian Museum, North Terrace, Adelaide, South Australia 5000, Australia; and [3]Mineral Sciences Department, Natural History Museum of Los Angeles County, 900 Exposition Boulevard, Los Angeles, CA 90007, USA

Abstract

Bimbowrieite, $NaMgFe_5^{3+}(PO_4)_4(OH)_6{\cdot}2H_2O$, is a new mineral found in a mineralogically zoned rare-element bearing pegmatite at the White Rock No.2 quarry, Bimbowrie Conservation Park, South Australia, Australia. Crystals are dark olive green to greenish brown and are bladed with dimensions of up to 150 μm. Crystals occur as aggregates up to 0.4 mm across associated with ushkovite, bermanite, leucophosphite and sellaite. Bimbowrieite is pleochroic, biaxial (+), with $\alpha = 1.785(5)$, $\beta = 1.795(5)$, $\gamma = 1.805(5)$ and 2V(meas.) = 89.4(5)°. The average of 28 chemical analyses gave the empirical formula: $(Na_{0.81}Ca_{0.19})_{\Sigma 1.00}(Mg_{0.75}Mn^{2+}_{0.19}Fe^{2+}_{0.05})_{\Sigma 0.99}(Fe^{3+}_{4.99}Al_{0.01})_{\Sigma 5.00}(PO_4)_{3.97}(OH)_{5.88}{\cdot}2.05\ H_2O$ based on 24 oxygen atoms. Bimbowrieite is monoclinic, space group $C2/c$ with $a = 25.944(5)$, $b = 5.1426(10)$, $c = 13.870(3$ Å, $\beta = 111.60(3)°$, $V = 1720.4(7)$ Å^3 and $Z = 4$. The crystal structure was refined to $R1 = 1.97\%$ for 1060 observed reflections with $F_o > 4\sigma(F_o)$. Bimbowrieite is isostructural with dufrénite. The structure is based on a trimer of face-sharing octahedra in which an *M*2 octahedra shares two *trans* faces with two *M*4 octahedra. Trimers link in the **c**-direction by sharing corners with two *M*3 octahedra and with *T*1 and *T*2 tetrahedra. Linkage in the **a**-direction is *via* corner-sharing *M*1 octahedra and linkage in the **b**-direction is *via* corner-sharing *T*1 and *T*2 tetrahedra.

Keywords: bimbowrieite; new mineral species; sodium magnesium iron phosphate; pegmatite; crystal structure; White Rock No.2 quarry; Australia

(Received 3 October 2023; accepted 3 November 2023; Accepted Manuscript published online: 13 November 2023; Associate Editor: Daniel Atencio)

Introduction

Minerals of the dufrénite group are known from many localities worldwide and occur as secondary minerals in a variety of environments; as late-stage minerals from hydrothermal alteration in granite pegmatites, in iron ore deposits and iron-rich gossans and in sedimentary phosphate deposits. The first crystal-structure investigation of minerals of the dufrénite group was completed by Moore (1970) who studied dufrénite from Cornwall, England. Other members of the dufrénite group (Table 1) are natrodufrénite (Fontan *et al.*, 1982), burangaite (Selway *et al.*, 1997), matioliite (Atencio *et al.*, 2006), gayite (Kampf *et al.*, 2010) and bimbowrieite. Structure analyses have been published on all except natrodufrénite. The general formula for dufrénite-group minerals may be written as $XM1M2M3M4(PO_4)_4(OH)_6{\cdot}2H_2O$ with Na and Ca at the *X* site, trivalent cations Fe^{3+} and Al at the *M*1, *M*3 and *M*4 sites and divalent cations Fe^{2+}, Mg and Mn^{2+} at the *M*2 site.

Corresponding author: Peter Elliott; Email: peter.elliott@adelaide.edu.au
Cite this article: Elliott P. and Kampf A.R. (2024) Bimbowrieite, $NaMgFe_5^{3+}(PO_4)_4(OH)_6{\cdot}2H_2O$, a new dufrénite-group mineral from the White Rock No.2 quarry, South Australia, Australia. *Mineralogical Magazine* **88**, 90–96. https://doi.org/10.1180/mgm.2023.86

The new mineral bimbowrieite is named for the Bimbowrie Conservation Park in which the type locality is located (see below). The mineral and name have been approved by the Commission on New Minerals, Nomenclature and Classification of the International Mineralogical Association (IMA2020-006, Elliott and Kampf, 2020). The holotype specimen is deposited in the collection of South Australian Museum, Adelaide, South Australia, Australia, registration number G34762.

Occurrence

The White Rock No.2 quarry from which the type specimen was collected is located in the Bimbowrie Conservation Park, 24 km N of Olary, South Australia, Australia. Pegmatites and pegmatoids are ubiquitous throughout the region, and occur as sills, dykes, lenses and segregation bodies of ill-defined shape (Campana, 1957). They have been intruded into rocks of the Archaean Willyama Complex. Willyama Supergroup rocks comprise upper greenschist- to amphibolite-grade metamorphosed and strongly deformed sedimentary and minor igneous rocks (Lottermoser and Lu, 1997), which are unconformably overlain by late Proterozoic Adelaidean metasediments. The White Rock pegmatite is one of more than 70 pegmatite bodies in the Olary Province of South Australia. It is a mineralogically zoned rare-element

Table 1. Comparison of related minerals.

Mineral name	bimbowrieite	dufrénite	natrodufrénite	gayite	burangaite	matioliite
Formula	$NaMgFe^{3+}_5(PO_4)_4(OH)_6{\cdot}2H_2O$	$Ca_{0.5}Fe^{2+}Fe^{3+}_5(PO_4)_4(OH)_6{\cdot}2H_2O$	$NaFe^{2+}Fe^{3+}_5(PO_4)_4(OH)_6{\cdot}2H_2O$	$NaMn^{2+}Fe^{3+}_5(PO_4)_4(OH)_6{\cdot}2H_2O$	$NaFe^{2+}Al_5(PO_4)_4(OH)_6{\cdot}2H_2O$	$NaMgAl_5(PO_4)_4(OH)_6{\cdot}2H_2O$
Space group	*C*2/c	*C*2/c	*C*2/c	*C*2/c	*C*2/c	*C*2/c
a (Å)	25.994(5)	25.84(2)	25.83(2)	25.975(3)	25.099(2)	25.075(1)
b (Å)	5.1426(10)	5.126(3)	5.150(3)	5.1766(4)	5.0491(7)	5.0470(3)
c (Å)	13.870(3)	13.78(1)	13.772(9)	13.929(1)	13.438(1)	13.4370(7)
β (°)	111.60(3)	111.20(6)	111.53	111.293(2)	110.88(1)	110.97(3)
V (Å^3)	1720.4(7)	1701.72	1703.94	1745.1(3)	1591.1(3)	1587.9(4)
Z	4	4	4	4	4	4
Reference	this work	Moore (1970)	Fontan *et al.* (1982)	Kampf *et al.* (2010)	Selway *et al.* (1997)	Atencio *et al.* (2006)

bearing pegmatite characterised by the occurrence of late-stage phosphate nodules between the quartz core and intermediate feldspar-rich zone and belongs to the beryl–columbite phosphate rare-element type in the classification of Černý (1991). Triplite–zwieselite was formed by metasomatic alteration of magmatic fluorapatite and has been transformed by hydrothermal alteration and weathering, in an oxidising, low-temperature, low-pH environment, to give a complex, microcrystalline intergrowth of secondary phosphate minerals (Lottermoser and Lu, 1997). At White Rock, three pegmatites with poor outcrops, up to 120 m long were mined for feldspar (both albite and microcline), muscovite and beryl over the period 1932–1973 (Olliver and Steveson, 1982). Three quarries were excavated to a depth of 10 m with recorded production of 860 tonnes of feldspar and 8.1 tonnes of beryl. Triplite and associated secondary phosphate minerals have been exposed in only the No.2 quarry. Bimbowrieite occurs in seams in a matrix comprising triplite and fluorapatite. Associated minerals are ushkovite, bermanite, leucophosphite and sellaite.

Appearance and physical properties

Bimbowrieite occurs as aggregates of crystals to 0.4 mm across (Fig. 1). Crystals are dark olive green to greenish brown blades, up to 150 μm in length. The blades are flattened on {100} and exhibit the crystal forms {100}, {111} and {201} (Fig. 2). The streak is olive green, the lustre is vitreous, the tenacity is brittle and the fracture is irregular. There is one excellent cleavage on {100}. Optically, bimbowrieite is biaxial (+), $\alpha = 1.785(5)$, $\beta = 1.795(5)$ and $\gamma = 1.805(5)$ (measured in white light). The $2V_z$ measured on a spindle stage is 89.4(5)°; the calculated $2V_z$ is 90.5°. Dispersion is $r < v$, extreme. The optical orientation is $Y = \mathbf{b}$, $X \wedge \mathbf{c} \approx 18°$ in obtuse β. The mineral is pleochroic with X = brown orange, Y = brown yellow, Z = blue green and $Y < X < Z$. The Gladstone–Dale compatibility index $1 - (K_P/K_C)$ for the empirical formula is 0.056 (good) (Mandarino, 2007).

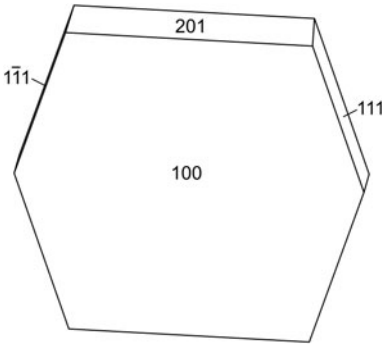

Figure 2. Crystal drawing of bimbowrieite (clinographic projection in standard orientation).

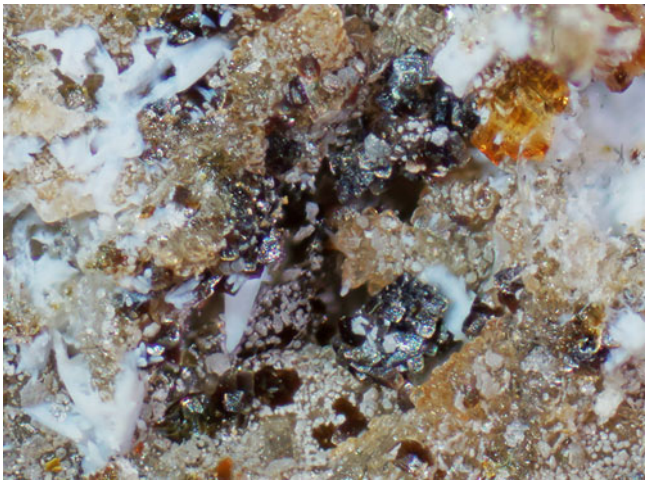

Figure 1. Greenish-brown crystals of bimbowrieite on fluorapatite, associated with ushkovite (orange) and sellaite (white). The field of view is 2.3 mm, South Australian Museum specimen G34762.

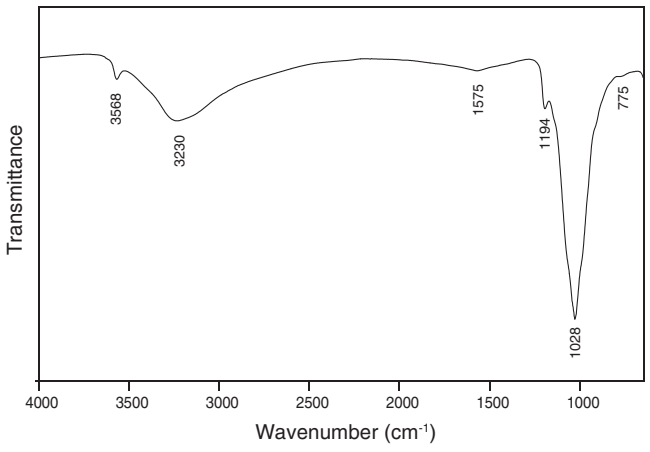

Figure 3. The FTIR spectrum of powdered bimbowrieite.

https://doi.org/10.1180/mgm.2023.86 Published online by Cambridge University Press

Table 2. Analytical data for bimbowrieite.

Constituent	Wt.%	Range	S.D.	Probe standard
Na_2O	2.93	2.29–3.49	0.27	albite
CaO	1.27	0.72–2.22	0.36	plagioclase
Al_2O_3	0.05	0.00–0.30	0.08	almandine–pyrope
Fe_2O_3*	46.90	45.36–47.13	0.47	almandine–pyrope
FeO*	0.45	0.00–1.81	0.66	almandine–pyrope
MgO	3.53	2.84–4.96	0.57	almandine–pyrope
MnO	1.56	0.76–2.70	0.65	rhodonite
P_2O_5	33.34	31.68–34.40	0.71	apatite
H_2O**	10.64			
Total	100.67			

*Fe_2O_3 and FeO calculated to give full occupancy of the *M*1, *M*3, and *M*4 sites by Fe^{3+}+Al.
**H_2O calculated from the crystal structure analysis.
S.D. = standard deviation

Infrared spectroscopy

The infrared spectrum (Fig. 3) of powdered bimbowrieite was recorded using a Nicolet 5700 FTIR spectrometer (range 4000 to 650 cm^{-1}, transmission mode) equipped with a Nicolet Continuum IR microscope and a diamond-anvil cell. The spectrum shows a broad absorption band due to OH stretching vibrations with maxima at 3568 cm^{-1} and 3230 cm^{-1}. According to the correlation given by Libowitzky (1999), the approximate O–H···O hydrogen bond-lengths range between 3.1 and 2.6 Å. A band found at 1575 cm^{-1} is assigned to the ν_2 H–O–H bending vibration of water molecules. The bands at 1194 and 1028 cm^{-1} may be assigned to the PO_4 ν_3 antisymmetric stretching vibrations and the band at 775 cm^{-1} is assigned to the PO_4 ν_1 symmetric stretching vibration.

Chemical composition

Quantitative chemical data were collected on two polished crystal aggregates using a Cameca SXFive electron microprobe (WDS mode, 20 kV, 20 nA, 5 μm beam diameter). Data were reduced using the ϕ(ρZ) method of Pouchou and Pichoir (1991). Twenty-eight points were analysed (Table 2). The small amount of material available did not allow for the direct determination of H_2O, so it was calculated give 10 H atoms per formula unit. The empirical formula, based on 24 O atoms, is $(Na_{0.81}Ca_{0.19})_{\Sigma 1.00}(Mg_{0.75}Mn^{2+}_{0.19}Fe^{2+}_{0.05})_{\Sigma 0.99}(Fe^{3+}_{4.99}Al_{0.01})_{\Sigma 5.00}(PO_4)_{3.97}(OH)_{5.88}\cdot 2.05\ H_2O$.

The ideal formula is $NaMgFe^{3+}_5(PO_4)_4(OH)_6\cdot 2H_2O$ which requires Na_2O 3.67, MgO 4.77, Fe_2O_3 47.27, P_2O_5 33.62, H_2O 10.67, total 100 wt.%.

X-ray crystallography and crystal-structure determination

Powder X-ray diffraction data (Table 3) were recorded using a Rigaku R-Axis Rapid II curved imaging plate microdiffractometer with monochromatised Mo*K*α radiation. A Gandolfi-like motion on the ϕ and ω axes was used to randomise the sample. Observed d values and intensities were derived by profile fitting using *JADE Pro* software (Materials Data, Inc.). The unit-cell parameters refined from the powder data using *JADE Pro* with whole-pattern fitting are: $a = 26.07(2)$, $b = 5.17(2)$, $c = 13.95(2)$ Å, $\beta = 111.56(2)°$ and $V = 1749(7)$ $Å^3$, which are in good agreement with the single-crystal study below.

A crystal was attached to a MiTeGen polymer loop and X-ray diffraction data was collected at the micro-focus macromolecular MX2 beamline at the Australian Synchrotron (Aragao *et al.*, 2018). Data were collected using a Dectris EigerX 16M detector

Table 3. Powder X-ray data for bimbowrieite. Only calculated lines with $I \geq 6$ are listed.

I_{obs}	d_{obs}	d_{calc}	I_{calc}	*h k l*	I_{obs}	d_{obs}	d_{calc}	I_{calc}	*h k l*	I_{obs}	d_{obs}	d_{calc}	I_{calc}	*h k l*
63	12.3	12.0839	30	2 0 0	43	2.640	2.6344	40	7 1 1	31	1.7369	1.7487	14	13 1 0
29	6.18	6.4578	7	0 0 2			2.5755	18	0 2 0			1.7354	17	$\bar{6}$ 0 8
		6.0420	15	4 0 0	14	2.489	2.4917	9	4 0 4			1.7263	21	14 0 0
100	5.04	5.0378	83	1 1 0	61	2.433	2.4499	10	$\bar{9}$ 1 3	16	1.6857	1.6806	14	7 1 5
		4.9834	35	2 0 2			2.4429	12	$\bar{3}$ 1 5	37	1.6610	1.6663	8	$\bar{1}$ 3 2
		4.8204	9	$\bar{1}$ 1 1			2.4265	16	5 1 3			1.6601	15	$\bar{8}$ 2 6
45	4.39	4.3847	21	$\bar{3}$ 1 1			2.4157	20	$\bar{5}$ 1 5			1.6560	18	$\bar{12}$ 2 2
		4.3397	9	3 1 0			2.4102	16	$\bar{2}$ 2 2			1.6445	11	$\bar{5}$ 1 8
56	4.12	4.1288	64	$\bar{1}$ 1 2			2.3747	14	3 1 4	36	1.6244	1.6304	14	$\bar{5}$ 3 1
		4.0280	21	6 0 0			2.3104	9	$\bar{9}$ 1 4			1.6281	6	$\bar{15}$ 1 4
		3.9867	10	$\bar{3}$ 1 2	11	2.297	2.2880	12	2 2 2			1.6155	23	$\bar{16}$ 0 4
15	3.807	3.7729	13	4 0 2			2.2301	6	1 1 5			1.6144	9	0 0 8
17	3.694	3.6591	30	$\bar{5}$ 1 1	15	2.165	2.1526	6	0 0 6	65	1.5858	1.5887	16	$\bar{10}$ 2 6
		3.5247	9	5 1 0			2.1471	6	$\bar{11}$ 1 2			1.5800	13	$\bar{5}$. 3 3
96	3.443	3.4527	26	$\bar{2}$ 0 4			2.1148	7	5 1 4			1.5777	56	2 2 6
		3.4189	19	$\bar{4}$ 0 4	59	2.119	2.1087	46	$\bar{11}$ 1 1			1.5739	9	$\bar{12}$ 0 8
		3.4137	66	$\bar{3}$ 1 3			2.1058	14	$\bar{5}$ 1 6			1.5541	9	$\bar{7}$ 2
93	3.234	3.2309	93	$\bar{8}$ 0 2	37	2.0661	2.0644	28	$\bar{2}$ 2 4	10	1.5296	1.5257	13	5 3 2
84	3.191	3.1774	100	$\bar{5}$ 1 3			2.0571	13	$\bar{4}$ 2 4	34	1.5056	1.5021	17	$\bar{12}$ 2 6
		3.1554	38	1 1 3			2.0482	7	3 1 5			1.5004	15	$\bar{14}$ 2 2
		3.0210	9	8 0 0	26	2.0171	2.0139	29	$\bar{8}$ 2 2			1.4997	7	$\bar{11}$ 1 4
56	3.011	3.0007	59	$\bar{7}$ 1 1			1.9961	11	2 0 6	15	1.4759	1.4906	8	$\bar{14}$ 2 4
		2.9811	10	$\bar{7}$ 1 2	29	1.9522	1.9599	8	8 2 0			1.4754	11	$\bar{9}$ 3 2
60	2.884	2.8784	70	$\bar{3}$ 1 4			1.9437	37	6 2 2			1.4676	7	15 1 1
		2.8679	31	7 1 0			1.9160	8	2 2 4	24	1.4568	1.4540	7	13 1 3
		2.8185	9	$\bar{1}$ 1 4	17	1.8545	1.8517	15	$\bar{5}$ 1 7			1.4510	11	$\bar{3}$ 1 9
		2.7943	15	5 1 2			1.8110	11	$\bar{11}$ 1 6					
		2.7737	7	$\bar{8}$ 0 4	23	1.7655	1.7657	9	11 2					
							1.7621	6	$\bar{8}$ 2 2					
							1.7581	10	$\bar{13}$ 1 5					

https://doi.org/10.1180/mgm.2023.86 Published online by Cambridge University Press

Table 4. Crystal data, data collection and refinement details.

Crystal data	
Space group	*C*2/c
a,*b*,*c* (Å)	25.944(5), 5.1426(10), 13.870(3)
β (°)	111.60(3)
V (Å^3), Z	1720.4(7), 4
F(000)	1685.0
μ (mm^{-1})	4.939
Absorption correction	multi-scan, T_{min}, T_{max}= 0.40, 0.43
Crystal dimensions (μm)	0.40 x 0.25 x 0.10
Data collection	
Diffractometer	Dectris EigerX 16M
Temperature (K)	100
Radiation	Synchrotron, λ = 0.710760 Å
Crystal detector distance (mm)	108.025
θ range (°)	1.69-23.15
h,*k*,*l* ranges	−26 → 26, −5 → 5, −14 → 14
Total reflections measured	6676
Unique reflections	1060 (R_{int} = 0.0352)
Refinement	
Refinement on	F^2
R_1 * for $F_o > 4\sigma(F_o)$.	1.97%
wR_2 † for all F_o^2	5.33%
Reflections used $F_o > 4\sigma(F_o)$	1057
Number of parameters refined	182
GooF	1.256
$(\Delta/\sigma)_{max}$	0.000
$\Delta\rho_{max}$, $\Delta\rho_{min}$ (*e*/Å)	0.350, −0.471

*$R_1 = \Sigma||Fo|-|Fc|| \,/\, \Sigma|Fo|$
†$wR_2 = \Sigma w(|Fo|^2-|Fc|^2)^2 \,/\, \Sigma w|Fo|^2)^{½}$; $w = 1/[\sigma^2(Fo^2) + (0.0177\ P)^2 + 7.86\ P]$;
$P = ([\text{max of } (0 \text{ or } F_o^2)] + 2Fc^2)/\ 3$

and monochromatic radiation with a wavelength of 0.710760 Å. The data set was processed using *XDS* (Kabsch, 2010) without scaling, and with absorption correction and scaling using *SADABS* (Bruker, 2001). Structure solution in space group C2/c was carried out using *SHELXT* (Sheldrick, 2015a) as implemented in the *WinGX* suite (Farrugia, 2012). The atom coordinates were then transformed to correspond to those in the structure of dufrénite (Moore, 1970). *SHELXL-2018* (Sheldrick, 2015b) was used for the refinement of the structure. All H atom sites were located in difference-Fourier maps and were refined with soft restraints of 0.82(3) Å on the O–H distances. The site occupancies at the *X* site and the *M*2 site were fixed to ($Na_{0.81}Ca_{0.19}$) and ($Mg_{0.75}Mn^{2+}_{0.19}Fe^{2+}_{0.05}$), respectively, in accordance with the electron microprobe data. The final refinement converged to an agreement index of R_1 = 1.97% for 1060 observed reflections with $F_o > 4\sigma$ (F_o). Data collection and refinement details are given in Table 4, atom coordinates and displacement parameters in Table 5, selected bond distances in Table 6 and a bond valence analysis in Table 7. The crystallographic information file has been deposited with the Principal Editor of *Mineralogical Magazine* and is available as Supplementary material (see below).

The main feature of the structure is a trimer of face-sharing octahedra, the "*h*-cluster" described by Moore (1970), which is also a feature in the structures of a number of other basic iron-phosphate minerals. A central $M2\phi_6$ octahedron shares two *trans* faces with two $M4\phi_6$ octahedra, via the OH5, O6 and O7 anions, to form a trimer of the form $[M_3\phi_{12}]$. Linkage in the **a**-direction is *via* corner-sharing *M*1 octahedra and *T*2 tetrahedra. Trimers link in both the **b**-direction and the **c**-direction by sharing corners with *M*3 octahedra and with *T*1 and *T*2 tetrahedra (Fig. 4).

The *X* site occupies channels that run along [010] and is coordinated by six O atoms and two H_2O molecules to form a square antiprism. The refinement yields an *X* site occupied by $Na_{0.84}Ca_{0.16}$ (12.43 epfu), in good agreement with the chemical analysis that shows $Na_{0.81}Ca_{0.19}$ (12.71 epfu). The bond-valence sum at the site of 1.34 is also in agreement with a mixed (Na, Ca) site population. Each of the *M* sites is coordinated by six anions in an octahedral arrangement. The *M*2 site is occupied by Mg plus minor Mn^{2+} and Fe^{2+} and is coordinated by four O anions and two OH groups. The site was refined with joint

Table 5. Fractional coordinates and displacement parameters (Å^2) for atoms for bimbowrieite.

	x	*y*	*z*	U_{eq}	U^{11}	U^{22}	U^{33}	U^{12}	U^{13}	U^{23}
X[a]	½	−0.1572(3)	¾	0.0073(7)	0.0053(10)	0.0096(10)	0.0064(10)	0	0.0013(6)	0
*M*1 (Fe)	½	0	½	0.0039(3)	0.0034(5)	0.0050(5)	0.0036(5)	−0.0010(3)	0.0015(3)	−0.0003(3)
*M*2 (Mg)[b]	¼	¼	0	0.0059(5)	0.0054(7)	0.0056(7)	0.0059(7)	0.0000(4)	0.0011(5)	−0.0003(4)
*M*3 (Fe)	0.34672(2)	0.01692(9)	0.38984(4)	0.0039(2)	0.0043(3)	0.0040(3)	0.0032(3)	−0.0010(2)	0.0012(2)	−0.0003(2)
*M*4 (Fe)	0.35947(2)	0.22512(10)	0.14906(4)	0.0041(3)	0.0041(4)	0.0039(4)	0.0041(4)	0.0001(2)	0.0012(2)	0.0000(2)
P1	0.28236(4)	0.73847(16)	0.16731(7)	0.0059(3)	0.0065(5)	0.0055(5)	0.0055(5)	−0.0001(4)	0.0022(4)	−0.0003(3)
P2	0.42124(4)	0.72423(17)	0.10846(7)	0.0065(3)	0.0066(5)	0.0059(5)	0.0071(5)	0.0006(4)	0.0029(4)	0.0002(3)
O1	0.42298(9)	0.4584(4)	0.15928(18)	0.0084(6)	0.0084(13)	0.0076(12)	0.0096(12)	0.0001(10)	0.0039(10)	0.0005(10)
O2	0.41124(10)	0.9366(5)	0.17786(17)	0.0092(5)	0.0095(12)	0.0078(12)	0.0096(12)	−0.0008(11)	0.0027(10)	0.0014(10)
O3	0.47861(10)	0.7800(5)	0.10190(18)	0.0107(6)	0.0081(14)	0.0125(13)	0.0112(13)	0.0043(10)	0.0033(11)	0.0008(10)
O4	0.37570(10)	0.7225(4)	0.00109(18)	0.0088(6)	0.0107(13)	0.0068(13)	0.0094(13)	0.0028(10)	0.0044(11)	0.0001(10)
OH5	0.32788(10)	0.2270(5)	−0.01339(18)	0.0086(6)	0.0121(14)	0.0076(13)	0.0082(13)	−0.0013(11)	0.0061(11)	−0.0009(10)
O6	0.29808(9)	0.5061(4)	0.11306(17)	0.0072(5)	0.0083(13)	0.0057(13)	0.0070(12)	−0.0012(10)	0.0021(10)	−0.0004(9)
O7	0.28974(9)	0.9921(4)	0.11435(17)	0.0076(6)	0.0089(13)	0.0066(13)	0.0061(12)	0.0003(10)	0.0014(10)	−0.0011(10)
OH8	0.37097(10)	0.2676(4)	0.29776(18)	0.0091(6)	0.0106(14)	0.0099(13)	0.0075(13)	0.0015(10)	0.0040(11)	0.0020(10)
O9	0.32327(10)	0.7443(4)	0.28071(18)	0.0084(6)	0.0091(13)	0.0099(14)	0.0049(12)	−0.0005(9)	0.0011(10)	0.0005(10)
O10	0.22295(10)	0.7095(5)	0.15877(18)	0.0095(6)	0.0080(13)	0.0113(13)	0.0100(13)	−0.0011(10)	0.0041(10)	−0.0008(10)
OH11	0.57579(9)	0.1352(5)	0.56802(18)	0.0105(6)	0.0073(13)	0.0086(14)	0.0142(13)	−0.0028(11)	0.0024(11)	−0.0001(10)
OH12	0.52308(10)	−0.2936(5)	0.60692(19)	0.0102(6)	0.0071(13)	0.0112(13)	0.0111(13)	0.0002(11)	0.0018(11)	−0.0019(11)
H5	0.338(2)	0.368(6)	−0.022(4)	0.050						
H8	0.3549(19)	0.405(7)	0.298(4)	0.050						
H11	0.579(2)	0.218(9)	0.619(3)	0.050						
H12A	0.5053(18)	−0.436(7)	0.594(4)	0.050						
H12B	0.5585(12)	−0.308(9)	0.634(4)	0.050						

[a]Refined occupancy $Na_{0.81}Ca_{0.19}$
[b]Refined occupancy $Mg_{0.75}Mn^{2+}_{0.19}Fe^{2+}_{0.05}$

https://doi.org/10.1180/mgm.2023.86 Published online by Cambridge University Press

Table 6. Selected interatomic distances (Å), angles (°) and hydrogen bonds for bimbowrieite.

X	*X*–OW12 ×2	2.380(3)	*M*3 (Fe)	*M*3–O10	1.951(2)	P1	P1–O10	1.509(3)
	X–O2 ×2	2.428(3)		*M*3–O4	1.972(2)		P1–O9	1.540(3)
	X–O1 ×2	2.475(3)		*M*3–O9	1.987(2)		P1–O7	1.543(2)
	X–O3 ×2	2.729(3)		*M*3–O5	2.024(2)		P1–O6	1.545(2)
	<*X*–O>	2.503		*M*3–O11	2.032(2)		<P–O>	1.534
				*M*3–O8	2.069(2)			
*M*1 (Fe)	*M*1–OH11 ×2	1.968(2)		<*M*–O>	2.015	P2	P2–O4	1.523(3)
	*M*1–O3 ×2	2.040(2)		BLD	1.786		P2–O1	1.531(2)
	*M*1–OW12 ×2	2.045(3)		OAV	14.522		P2–O2	1.540(3)
	<*M*–O>	2.018					P2–O3	1.551(3)
	BLD	1.641	*M*4 (Fe)	*M*4–O2	1.941(2)		<P–O>	1.536
	OAV	7.203		*M*4–OH8	1.984(2)			
				*M*4–O1	2.000(2)			
*M*2 (Mg)	*M*2–O7 ×2	2.033(2)		*M*4–O6	2.071(2)			
	*M*2–O6 ×2	2.076(2)		*M*4–O7	2.073(2)			
	*M*2–OH5 ×2	2.099(2)		*M*4–OH5	2.095(2)			
	<*M*–O>	2.069		<*M*–O>	2.026			
	BLD	1.171		BLD	2.581			
	OAV	140.916		OAV	63.585			

Hydrogen bonds *D*–H···*A*	*D*–H	H···*A*	*D*···*A*	∠*D*–H···*A*
OH5–H5···O4	0.79(3)	2.04(3)	2.809(3)	163(5)
OH8–H8···O9	0.82(3)	1.90(3)	2.717(3)	169(5)
OW12–H12A···O1	0.85(3)	2.61(5)	3.062(3)	115(4)
OW12–H12A···O3	0.85(3)	1.92(3)	2.745(3)	165(5)
OW12–H12B···OH8	0.86(3)	1.74(3)	2.578(4)	166(5)

Note: BLD = bond-length distortions (Renner and Lehmann, 1986); OAV = octahedral angle variance (Robinson *et al.*, 1971).

occupancy by Mg and Mn, yielding a site-scattering value of 16.32 e^-. This is greater than the site-scattering value of 15.17 e^- based on the site occupancy indicated by the empirical formula. The most likely explanation is that the crystal used for the structure determination was higher in Mn and lower in Mg than the crystal used for electron probe microanalysis (EPMA). The large variations in these elements noted during the EPMA further support this explanation. Fe^{3+} occurs at three symmetrically distinct sites, *M*1, *M*3 and *M*4. The *M*1 site is coordinated by two O atoms, two OH groups and two H_2O groups. The *M*3 site is coordinated by three O atoms and three OH groups and the *M*4 site is coordinated by four O atoms and two OH groups. The observed mean *M*–ϕ bond-lengths for the *M*1, *M*3 and *M*4 sites (2.018, 2.015 and 2.026 Å respectively) and bond-valence sums (Table 7) support the occupancy of the *M*1 site by Fe^{3+} plus minor Al. This is in agreement with the structure refinements of other members of the dufrénite group in which the smaller *M*1, *M*3 and *M*4 octahedral sites are dominated by either Fe^{3+} or Al. Of the *M* sites, *M*3 and *M*4 are more distorted in terms of bond-length distortion (BLD) and *M*2 and *M*4 are more distorted in terms of octahedral angle variance (OAV) (Table 6). Two symmetrically distinct sites, P1 and P2 in the structure are fully occupied by P. The PO_4 tetrahedra show similar <P–O> distances and degrees of geometrical distortion.

There are three OH groups and one H_2O group in the structure. The hydrogen bonding scheme (Table 6) for bimbowrieite is the same as that reported in previous studies on the dufrénite-group minerals burangaite (Selway *et al.*, 1997) and matioliite (Atencio *et al.*, 2006). The OH5 and OH8 groups provide hydrogen bonds accepted by O4 and O9, respectively. OW12

Table 7. Bond valence* (vu) sums for bimbowrieite.

	X	*M*1	*M*2	*M*3	*M*4	P1	P2	H5	H8	H11	H12A	H12B	Sum
O1	0.17×^{2}↓				0.55		1.23					0.10	2.05
O2	0.19×^{2}↓				0.62		1.26						2.07
O3	0.09×^{2}↓	0.46×^{2}↓					1.20				0.20		1.95
O4				0.56			1.28	0.17					2.01
OH5			0.37×^{2}↓	0.49	0.43			0.83					2.12
O6			0.35×^{2}↓		0.40	1.21							1.96
O7			0.41×^{2}↓		0.43	1.22							2.06
OH8				0.43	0.52				0.80			0.18	1.93
O9				0.54		1.23			0.20				1.97
O10				0.60		1.32							1.92
O11		0.57×^{2}↓		0.48						1.00			2.05
OW12	0.22	0.47×^{2}↓									0.80	0.72	2.21
Sum	1.34	3.00	2.26	3.10	2.95	4.98	4.97	1.00	1.00	1.00	1.00	1.00	

*Bond-valence parameters used are from Gagné and Hawthorne (2015).
Bond valences for the *X* and *M*(2) sites are based on the refined occupancy.

https://doi.org/10.1180/mgm.2023.86 Published online by Cambridge University Press

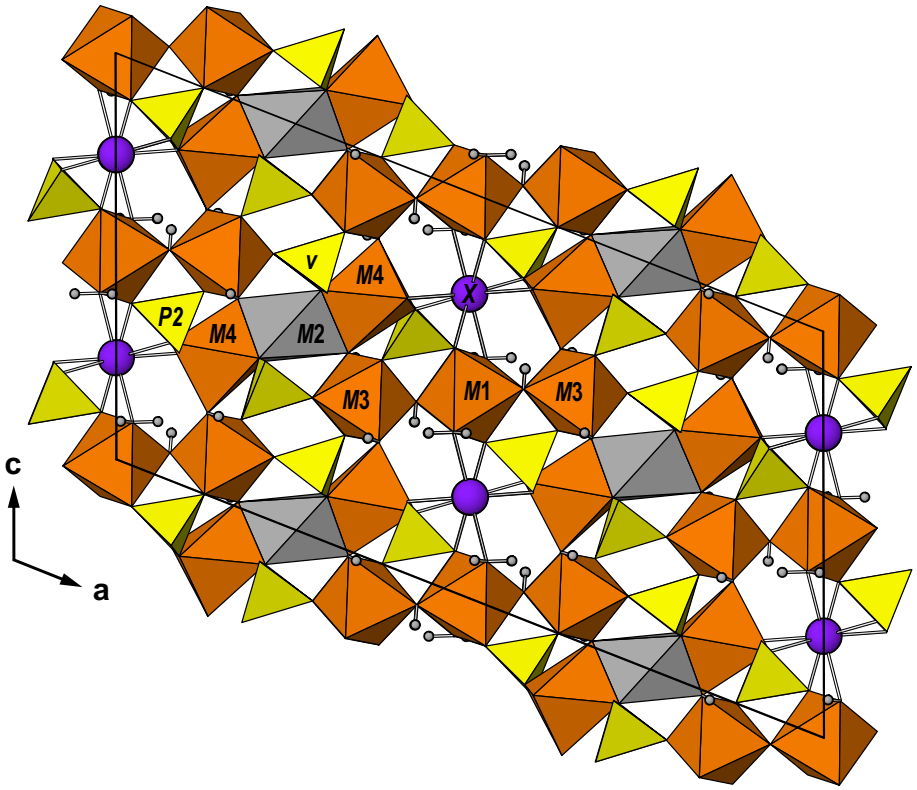

Figure 4. The crystal structure of bimbowrieite viewed along [010]. Hydrogen atoms are small grey spheres. The unit cell is outlined.

provides three hydrogen bonds accepted by O1, O3 and OH8. The hydrogen bonds are of weak to medium strength with O–O distances in the range 2.580 to 3.065 Å.

Acknowledgements. The authors thank Ben Wade of Adelaide Microscopy, The University of Adelaide for assistance with the microprobe analysis. The infrared spectrum was acquired with the assistance of the Forensic Science Centre, Adelaide. This research was undertaken in part using the MX2 beamline at the Australian Synchrotron, part of ANSTO, and made use of the Australian Cancer Research Foundation (ACRF) detector.

Supplementary material. The supplementary material for this article can be found at https://doi.org/10.1180/mgm.2023.86.

Competing interest. The authors declare none.

References

Aragao D., Aishima J., Cherukuvada H., Clarken R., Clift M., Cowieson N.P., Ericsson D.J., Gee C.L., Macedo S., Mudie N., Panjikar S., Price J.R., Riboldi-Tunnicliffe A., Rostan R., Williamson R. and Caradoc-Davies T.T. (2018) MX2: a high-flux undulator microfocus beamline serving both the chemical and macromolecular crystallography communities at the Australian Synchrotron. *Journal of Synchrotron Radiation*, **25**, 885–891.

Atencio D., Coutinho J.M.V., Mascarenhas Y.P. and Ellena J.A. (2006) Matioliite, the Mg-analog of burangaite, from Gentil mine, Mendes Pimentel, Minas Gerais, Brazil, and other occurrences. *American Mineralogist*, **91**, 1932–1936.

Bruker (2001) *SADABS*. Bruker AXS Inc., Madison, Wisconsin, USA.

Campana B. (1957) Granites, orogenies and mineral genesis in the Olary Province (South Australia), *Journal of the Geological Society of Australia*, **4**, 1–12.

Černý P. (1991) Rare element granitic pegmatites, part I. Anatomy and internal evolution of pegmatite deposits. *Geoscience Canada*, **18**, 49–67.

Elliott P. and Kampf A.R. (2020) Bimbowrieite, IMA 2020-006. CNMNC Newsletter No. 55; *Mineralogical Magazine*, **84**, https://doi.org/10.1180/mgm.2020.39

Farrugia L.J. (2012) WinGX and ORTEP for Windows: an update. *Journal of Applied Crystallography*, **45**, 849–854.

Fontan F., Pillard F. and Permingeat F. (1982) La natrodufrénite (Na,□)(Fe^{+++},Fe^{++})(Fe^{+++},Al)$_5$(PO_4)$_4$(OH)$_6$·2H_2O, une nouvelle espèce minérale du groupe de la dufrénite. *Bulletin de Minéralogie*, **105**, 321–326.

Gagné O.C. and Hawthorne F.C. (2015) Comprehensive derivation of bond-valence parameters for ion pairs involving oxygen. *Acta Crystallographica*, **B71**, 562–578.

Kabsch W. (2010) XDS. *Acta Crystallographica*, **D66**, 125–132.

Kampf A.R., Colombo F. and González del Tánago J. (2010) Gayite, a new dufrénite-group mineral from the Gigante granitic pegmatite, Córdoba province, Argentina. *American Mineralogist*, **95**, 386–391.

Libowitzky E. (1999) Correlation of O-H stretching frequencies and O–H···O hydrogen bond lengths in minerals. *Monatshefte für Chemie*, **130**, 1047–1059.

Lottermoser B.G. and Lu J. (1997) Petrogenesis of rare-element pegmatites in the Olary Block, South Australia, part 1. Mineralogy and chemical evolution. *Mineralogy and Petrology*, **59**, 1–19.

Mandarino J.A. (2007) The Gladstone-Dale compatibility of minerals and its use for selecting mineral species for further study. *The Canadian Mineralogist*, **45**, 1307–1324.

Moore P.B. (1970) Crystal chemistry of the basic iron phosphates. *American Mineralogist*, **55**, 135–169.

Olliver J.G. and Steveson B.G. (1982) Pegmatites in the Olary Province. A review of feldspar and beryl mining north of Olary and the results of reconnaissance sampling of feldspar. *Report 81/74. South Australian Department of Mines and Energy*, Adelaide, Australia.

Pouchou J.-L., and Pichoir F. (1991) Quantitative analysis of homogeneous or stratified microvolumes applying the model "PAP". Pp. 31–75 in: *Electron Probe Quantitation* (K.F.J. Heinrich and D.E. Newbury, editors). Plenum Press, New York.

Renner B. and Lehmann G. (1986) Correlation of angular and bond length distortions in TO_4 units in crystals. *Zeitschrift für Kristallographie*, **175**, 43–59.

Robinson K., Gibbs G.V. and Ribbe P.H. (1971) Quadratic elongation; a quantitative measure of distortion in coordination polyhedra. *Science*, **172**, 567–570.
Selway J.B., Cooper M.A. and Hawthorne F.C. (1997) Refinement of the crystal structure of burangaite. *The Canadian Mineralogist*, **35**, 1515–1522.
Sheldrick G.M. (2015a) SHELXT – Integrated space-group and crystal-structure determination. *Acta Crystallographica*, **A71**, 3–8.
Sheldrick G.M. (2015b) Crystal structure refinement with SHELXL. *Acta Crystallographica*, **C71**, 3–8.

https://doi.org/10.1180/mgm.2023.86 Published online by Cambridge University Press